

# Nanostructured Alloys for High-Temperature Applications: A Study on Performance and Longevity

Sairam M

Department of Mechanical Engineering

SSN College of Engineering

Rajiv Gandhi Salai (OMR)

Kalavakkam, Chennai, Tamil Nadu, India – 603110

ssairm@gmail.com

## Abstract

Nanostructured alloys have become a revolutionary material for high-temperature applications due to their exceptional mechanical properties, thermal stability, and resistance to environmental degradation. The present work focuses on the performance and durability of these materials with respect to extreme conditions in advanced engineering systems. Nano-oxides, for instance, Y<sub>2</sub>Ti<sub>2</sub>O<sub>7</sub> pyrochlore have been found to play an essential role in optimizing creep resistance and tensile strength and also showing improved irradiation tolerance, thus finding applications in the fusion and fission reactors. Though significant amounts of progress in understanding the routes of composition processing to optimize properties have been accomplished, fabrication remains a difficult step in achieving reproducible performance because of defect introduction. This study also assesses the economic and practical feasibility of using nanostructured alloys in critical high-temperature environments, providing insight into their long-term reliability and potential for transformative industrial applications.

**Keywords:** Nanostructured alloys, High-temperature applications, Thermal stability, Nano-oxides, Irradiation resistance and Advanced engineering systems.

## 1.Introduction

In this current era, there is a necessity to have cutting-edge, high-performance construction components that are capable of safely supporting a longer ingredient lifetime in very hostile settings in order to effectively produce new large-scale, carbon-free Gen IV uranium technologies and subsequent forms of energy that are based on fusion. The presence of circumstances such as high temperatures, considerable time-dependent stresses, chemically active cooling agents, and intense radiation flows are examples of particular examples of these states [1] nm-scale dispersoids, which are durable over lengthy neutron service at extreme temperatures, have the potential to be both very powerful and possess a distinct irradiation sensitivity, according to a number of research that were carried out in the succeeding years [2]. Several arrangements involving nm-scale phases and hosting metallic sheets offer appealing microstructures as such as steels, nickel, titanium as a metal aluminium, and refractory metal alloys. Austenitic metals, heat-treatable 9Cr ferritic martensitic, and greater Cr completely

ferritic alloys have all been strengthened via nanodispersion. The alloy carbonitrides and oxides are the main constituents of the dispersoids [3]. Machining options include powder metallurgy approaches and variations of traditional melt-thermomechanical procedure.

The contents of this Discussion Newspaper will focus on the current state of so-called nanotechnology ferritic metals (NFAs), which are an a category of oxide distributing solidified (ODS) steels. This is due to the fact that NFAs have a wide range of applications and there is a rapidly growing interest in this category of components all over the world. The selection was reached for a variety of reasons, however one may argue that non-functional components (NFAs) provide the most daunting challenges in addition to the greatest promise, at least for some significant applications such as first wall fusion architectures. Cr-12-16% Fe-12 Extraordinary long-term temperature tolerance up to over 900 degrees Celsius, exceptionally high tensile, fatigue, and creep capabilities throughout a wide range

of temperatures thereby and extraordinary radiation compassion, especially when dealing with high nitrogen concentrations are all characteristics of non-ferrous alloys (NFAs). NM-scale nano-oxides (NOs) that provide a superb set of mechanical and functioning the characteristics are directly or indirectly responsible for their extraordinary capacities. These nano-oxides have low elements of the volume (f order 0.5%) of ultrahigh numerical densities (N order  $5 \times 10^{23} / \text{m}^3$ ). On average, the d order of nano-oxides is 2.5 nm. There are further characteristics of NFA microscopy such as a high number of dislocations and grains that are smaller than a micron. The NOs are typically Y-Ti-O centred phases, despite the fact that different components from Groups 4 and 3 may be utilised to replace Ti (Zr and Hf) and Y (Sc).

The modified martensitic metal (TMS) form of ODS metals having 9Cr and C shares many of the same principles as NFAs. When it comes to material for engineering, ODS TMS are much more advanced than NFA, especially when it comes to fabrication. Additionally, highly corrosion and oxidation resistant Al bearing iron steels are desirable options for environmentally demanding environments and accident-tolerant cladding, but they often suffer from the substitution of coarser scale Al-Y oxides for the fine Y-Ti-O NOs. The oxide dispersion strengthening (ODS) and Al alloyed steels, however, will not be treated in greater depth here due to the manuscript's length restriction; nonetheless, they are noteworthy for being thoroughly reviewed in a recent study [4].

The technical domains of homogeneity, fabricability, submitting, expense, and commercial manufacturing capacity now pose the biggest obstacles to the practical development of NFAs. The purpose of this work is not to provide a review [5,6] There aren't enough references—that would be impossible. They consist of three important PhD theses that include content that wouldn't otherwise be widely distributed as well as helpful reviews. Though solely the author's responsibility, the opinions presented here try to represent a broader consensus among these exceptional scholars, and the author is grateful for their very helpful suggestions.

The primary emphasis of the study is on the fundamental NFA materials science challenges, which include microstructure, mechanical characteristics, irradiation tolerance, heat and ultraviolet equilibrium, and NFA manufacturing. In this context, it is not feasible to fully discuss the complicated complexities and difficulties associated with plasticity processing and integrating

NFA bits due to length limits; as therefore, these issues are just addressed in passing [7]. In conclusion, a short discussion is held on the significant and more general concerns of allowing factor in composite element frameworks for fission power nuclear reactors, specifically fusion power breeders. Contributions of the Study are,

- It discusses how nanostructured ferritic alloys (NFAs) function in terms of withstanding high temperature, radiation, and strength properties under extreme conditions.
- It mentions the key obstacles that are creating a barrier towards the widespread usage of NFAs, including some manufacturing problems, cost, and uniform quality.
- The study assesses how NFAs can be applied in future energy systems, such as fusion and fission reactors, to prove their capability to function effectively under harsh conditions.

## **2. The Physical and Chemical Science of Non-Ferrous alloys**

### **A. Powder metallurgy, processing pathways, and structure**

Intensive grinding with ball mills is often used to mechanically amalgam rapidly generated Fe-Cr-Ti-W powders with tiny quantities of  $\text{Y}_2\text{O}_3$ . This is done with the aim to disintegrate the Y that was previously resistant to chemical reactions and to add additional components of oxygen. Lattice-trapping Y by rapid powder solidifying fails because of  $\text{Y}_2\text{Fe}_{17}$  intracellular phase separation. For nm-scale metals to develop, the right O and Ti levels are essential. To create ultrafine,  $\approx 2\text{-}3$  nm dimension  $\text{Y}_2\text{Ti}_2\text{O}_7$  pyrochlore complexes NOs, the amount of oxygen must be greater than that brought about by  $\text{Y}_2\text{O}_3$  on its own, and Ti should be balanced. Basic mechanics and kinetics pertaining to phase select and dissolution scales drive this alloy formula. Oxygen may be added due to quick solidification, contaminant collection, or ball milling with Fe-oxides.

Y can additionally be introduced by other substances that include Group 4 elements, such as hydroxides [8,9]. In general, N contaminant interference and unprocessed Ti and O in fine-scale Y-Ti oxides must be avoided. The molecular content of the fine NOs scales proportionally with the alloy Y concentration when the chemical formulas are appropriately matched. During powder combining, NO deposition occurs very quickly, yet it exhibits traditional C-curve temperature kinetics [10–12], with a peak at around  $650^\circ\text{C}$ . N and f drop under



normal consolidation circumstances, which are between 850 and 1150°C, whereas  $d$  rises as temperature rise. In properly prepared NFAs, the NOs are rather evenly spread across the matrix and also develop on borders of grains, where they are a little bigger [13].

Additionally, size distribution and crystalline structuring are additional essential aspects for integrating NFA small structures. This can be observed in the electromagnetic reflections irradiation (EBSD) inversion pole figures map shown in Figure 1a for an extrusion and cross-rolled NFA sheets with pancake-shaped nanoparticles. The top come to rest, also known as width introductions, of the strong texture indicates that the majority of the planes that are perpendicular to the edges of the structure total one hundred. A significant  $\langle 011 \rangle$ -fiber texture is shown when extensions and cross rollers views (front and side portions) are seen. An intriguing observation is that the bcc  $\{100\}\langle 011 \rangle$  system has a very low cleavage endurance in the presence of iron, which results in the formation of minute fractures in the cross-rolling orientated perspective (as seen in white on the laterally portion of Figure 1)

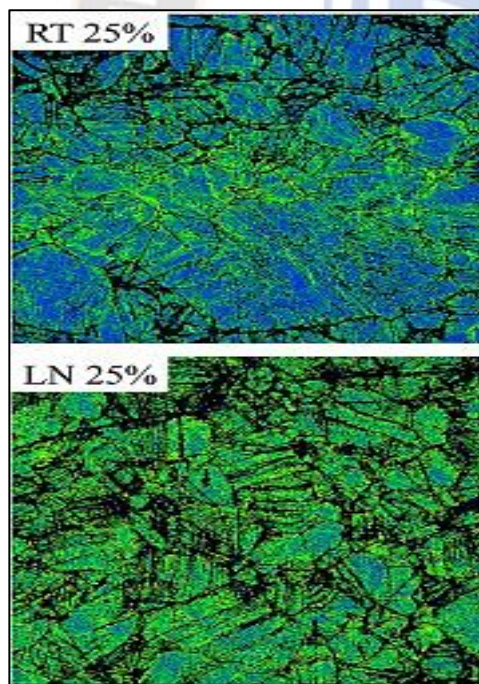


**Figure 1: The bidirectional pore size transportation, the (100) plane, the  $\langle 110 \rangle$ -fiber shaping, and the**

**existence of a microcrack are all visible within Figure 1's (a) multidimensional electron backwards diffraction (EBSD) maps and (b) SEM photographs of a portion of the NFA sheet. Keep in mind that the different perspectives are not consistent with one another in all three planes since they are not for the identical spot on the plate.**

The NFA grain size distributions are generally bimodal, which is with a much smaller number of bigger grains reaching up to greater than 10  $\mu\text{m}$  but a preponderance of tiny a submicron particles (averaging  $\approx 500$  nm in Fig. 1). The NOs are dispersed in both big and tiny grains, unlike what was previously thought. Large variations in the ultra-high displacement densities in the milling powdered are probably what cause certain grains to develop; these stresses on grain boundaries, particularly before the NOs has completely accumulated, considerably outweigh Zener pinning pressures. There are less bigger particles and smaller finer grains as a consequence of fewer degrees Celsius consolidation.

#### **B. Characteristics of NOs and Their Interfaces with Ferrite Matrix**

The nitrogen oxides (NO) were thought to be cohesive sub-oxide transitioning phases that were concentrated in Ti and O but contained very little Y and a lot of Fe, according to earlier atom probe radiography investigations. It is now generally acknowledged that a number of APT artefacts led to this result. In addition, the TEM observations revealed that the NO were either granulated or TiO-dominated complexes with salt-like structures. This was observed by the researchers themselves. On the other hand, here is now universal consensus that, in a large number of cases, the lesser NOs indicate the fcc  $\text{Y}_2\text{Ti}_2\text{O}_7$  pyrochlore period. This conclusion depends on a substantial and expanding body of transmitting electron microscopy (TEM) data as well as more limited x-ray investigations. For instance, Fig. 2a displays a  $1.8 \times 3.6$  nm  $\text{Y}_2\text{Ti}_2\text{O}_7$  NO. While bigger  $\text{Y}_2\text{Ti}_2\text{O}_5$  oxidation have been found in NFAs [14,15], the oldest and tiniest oxides and their putative development from precursors to the pyrochlore architecture remain unclear.

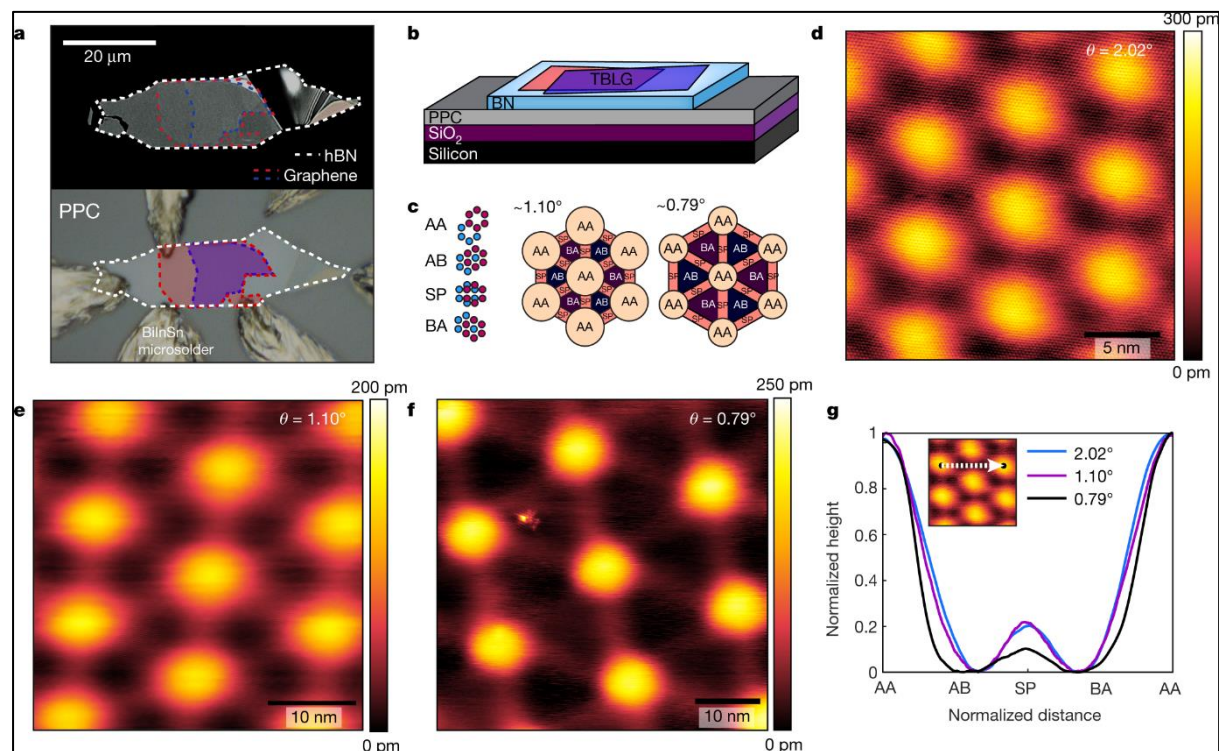


**Figure 2:** - a) 1.8 x 3.6 nm Y<sub>2</sub>Ti<sub>2</sub>O<sub>7</sub> NO with Moire borders from consistency types; b) STEM and c) exit wave focal series pictures of a larger Y<sub>2</sub>Ti<sub>2</sub>O<sub>7</sub> NO, exposing its ordered pyrochlore framework and 5x7 near-coincidence site lattice interface with the Fe-Cr the matrix; d) Fe and Y<sub>2</sub>Ti<sub>2</sub>O<sub>7</sub> cell units and position. e) Raw HRSTEM, f) rectified picture, and g) 3-D polyhedral depiction of a NO.

Naturally, NFAs depend heavily on the oxide-ferrite connections, particularly on NOs' capacity to capture and hence control helium. Consequently, interface architecture and orienting connections (ORs) have received a lot of attention. For instance, as with the bigger oxide with a 5x7 Fe near coincidental site structure in Figs. 2b and 2c, the wide 1.8 nm boundary in Fig. 2a is cubed on edge. The Y, Ti, and Y + Ti arrangement of the pyrochlore molecular column could be seen in this instance.

Fig. 2d shows the unit cells and interface ORs for the NO in Fig. 2a. As can be seen from the Moiré edges in Fig. 2a, these interfaces are consistent and impose significant crystalline stresses. The interfaces exhibit semicoherent as well as separate misfit displacement structures at even greater scales, as is additionally the case with Fe-Y<sub>2</sub>Ti<sub>2</sub>O<sub>7</sub> meso-scale dual layers. Lastly, a raw TEM picture of a NO that includes two connected bubbles (depicted in Fig. 2f) is shown in Fig. 2e.

NOs are truly three-dimensional, multifaceted polygons, as shown in Fig. 2g, and as a structural requirement, they need a variety of low indices oxide-matrix interactions. Notably, NO bubble production preferentially occurs on the tiny {111} corner facets, as seen in Fig. 2g.

### C. Kinetics and the thermodynamics: stage selection, interfacial energy, precipitating, and thermal stability.

There is a significant disparity in energy between the bulk periods that contained the substances directly and those that are disseminated around the framework. Furthermore, there are large decreases in energy that take place when the earliest stages of solute Y-Ti-O clumping. It is possible that this is the most important aspect of mechanics that pertains to NO snowfall. With the use of climatic data and calculations based on basic principles, phase diagrams have been developed that illustrate oxide preference as an indicator of temperature, alloy dissolving O concentrations (represented by relative pressure, or PO<sub>2</sub>), and the ratio of titanium to yttrium [16]. It is anticipated that the compounds in question will be a combination of Y<sub>2</sub>Ti<sub>2</sub>O<sub>7</sub> and Y<sub>2</sub>TiO<sub>5</sub> at all PO<sub>2</sub> levels above about 10-28 atm at a temperature of 1000°C, and for Ti/(Y+Ti) ratios ranging between 0.35 and 0.5 [17]. In general, this mix range reduces the amount of undesirable TiO<sub>2</sub> and avoids the formation of Y<sub>2</sub>O<sub>3</sub> whether the Ti content is lower or greater. The advice for alloy design that these predictions give are helpful, and they are typically in accord with observations received.



It has been shown via the use of density-functional theory (DFT) and kinetics calculations [18] that the NO interface energy ( $\gamma$ ) exhibits a significant degree of reactivity in relation to the local ending geometry and PO<sub>2</sub>. In a general sense, the kinetic energy of proper interfaces is substantially greater than the potential of anion or cation enriched interactions. In addition, when the concentration of PO<sub>2</sub> is quite low, cation-rich surfaces are selected for use in homeostatic with Fe compounds. In this case, the  $\gamma$  decreases as the PO<sub>2</sub> decreases. As a matter of fact, however, the quantity of non-equilibrium soluble oxygen may be far higher, which may lead to surfaces that are rich in oxygen yet have energies that decrease as the quantity of PO<sub>2</sub> increases. It is estimated that the effective contact radiation of the NO ferrite will be less than one joule per square metre in any of the two scenarios. In accordance with the clustering method, an interface that has an energy of around 1 J/m<sup>2</sup> and PO<sub>2</sub> that is in equilibrium with CrO<sub>2</sub> corresponds with the observed increase of NO throughout the process of synthesis and thermal ageing, which ultimately leads to a gradual accumulation of NO. The Y<sub>2</sub>Ti<sub>2</sub>O<sub>7</sub> NOs have very high thermal conductivity. The NOs will remain practically stable for many thousands of hours up to more than 900°C, according to long-term, high temperatures thermal ageing studies [19]. NO constancy is not caused by Y's slow diffusion rate, as some have argued. Rather, sluggish elevated NO the coarsening kinetics is caused by inadequate Y absorbing in local homeostasis with Y<sub>2</sub>Ti<sub>2</sub>O<sub>7</sub>. Indeed, pipe dissemination along dislocations—where Y is more fluid and moves faster compared in the matrix—coarsens. The dislocated pipe dissolution-diffusion coarsening process exhibits high efficient activation power of about 673 kJ/mole and  $\approx t^{1/5}$  kinetics. Keep in mind that, for at least tens of thousands of hours, the grain sizes and deformation concentrations remain constant at 950°C.

#### **D. Mechanical Characteristics**

NFAs often exhibit notable plasticity in addition to exceptional tensile, creep, and fatigue resilience. The room ambient compressive yield value for NFAs ranges greatly, from close to 600 to 1600 MPa, as shown in Fig. 3a. Despite their high strength, NFAs exhibit tensile

flexibility and high stress hardening rates, with SM10 alloys (red circles) exhibiting 2% total extension and NFA-1 (blue rectangles) exhibiting 8%. Although they fluctuate with NFA temperatures, the creep ductility and toughness are typically significant, allowing for 40,000 hours of operation up to 800°C at pressures of ordering 100 MPa. Although there are differences in the published specifics of NFA creep behaviour, it is generally observed that there are no notable tertiary creep tensions. Although fundamental creep stress are often small at low loads, they should be given more consideration since they might be important in particular applications. According to certain unreleased French statistics, NFA does not seem to have a prolonged maximum creep rates regime (Y. De Carlan). In addition, NFAs have a considerably higher fatigue strength than traditional 9Cr-type TMS, and neither NFAs nor ODS steels undergo cyclic strain softening.

The total NFA microstructures as not just the NOs, are responsible for the exceptional strength and ductility. In fact, the extremely tiny grain size HallPetch hardening may contribute more to cold-temperature strength than the NOs, based on the alloy in question. The processes behind building up at lower temperatures are rather well known and modelled. Over 400°C, the cracking mechanism in NFAs changes to viscoplastic creep (see Fig. 3a). Various creep illustrations have been presented, but the most important identifying is that movement creep in NFAs is regulated by a high effective threshold attained nervousness, resulting in quite a bit of the static stress field and causes highly elevated strain rate and fragmenting time anxiety exponentiation. NFA diffusion creep levels are small, but additional study is required. Formed NFAs' creep characteristics are strongly influenced by orientation. Transverse creep and flexibility in tubing are considerably less than in the extrusion-axial plane. Therefore, heat procedures for recovery and recrystallisation are often required to increase fabricability as well as transversal ductility and stiffness[20]. However, recovery and recrystallisation give up some of the benefits of high NFA strength while homogenising its structural characteristics. The development of heat processes that equalise NFA characteristics and fabricate NFA components is still ongoing (see below).

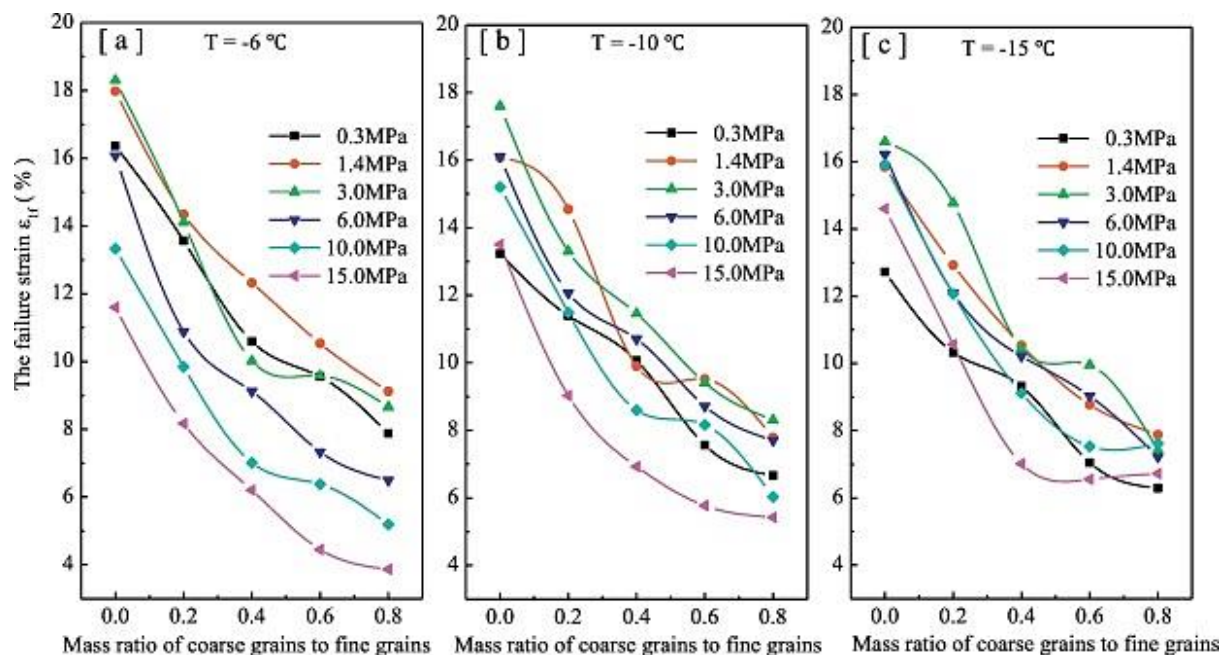


**Figure 3: a) The yield stresses of different NFA levels exhibits a fairly broad spectrum of behaviour as a function of temp. b) The fracture toughness of different NFA the temperature as a function of temperatures exhibits a very broad range of behaviour, as well as the impact of sample position; take note that the stretching strategy toughness is typically much lower (TL and CL), whereas all of the the literary genre's excellent toughness findings are for the stronger transverse crack deflecting (LT and LR) orientations. b) A example ductile tearing load dispersion curve with typical photos of the delaminations that formed during tests at  $-175^{\circ}\text{b}$  for T-L orientations and  $-150^{\circ}\text{C}$  for T-S directions**

In applications that tolerate defects, the impact of cracks and defects on NFA breakage limitations have to be considered. NFAs' high strength values lead to a wide range of fracture resilience  $\text{KJc}$ , as seen in Fig. 3b, as well as high brittle-to-ductile fracture temperature transitions (BDTT). NFAs often, but not always, have extremely asymmetric fracture resilience and impact resistance characteristics. Cracks travelling in the primary displacement directions—represented by the filled symbols—have a weaker configuration for quick fracture. The weak transversal inclination for creep is exactly the reverse of this. When cracks propagate transversely, as shown by blank arrows in Fig. 3b,  $\text{KJc}$  is often greater.

As demonstrated in Fig. 3c, steady crack propagation occurs in this instance due to ductile tearing, which is followed by a slow and elegant decrease in load. Large-scale delaminations are the cause for the rupture of ductility mechanism, which are likewise shown in Fig. 3c, are caused by the plate's accumulation of microcracks, as seen in Fig. 1. The triaxial breaking tip pressures in the brittle, undamaged links connecting the delaminations are too small to promote cleavage flexible tear. When fractures propagate throughout the plate

width, normal breaks in installation and cross rolled layouts,  $90^{\circ}$  fracture dislocation and Type II propagation within the delaminations boost durability.

A NFA fractured body's significant effective strength as well as flexibility are shown by sustained crack tearing load-displacement curve. Flexible shredding might not constitute a major fail reason for several structures, hence total uncracked segmental tension may be used instead of fractured force. Because ductile tearing often follows general breaking down, the yielding and flowing stresses also drop, which lowers the highest ripping load below ambient temperature. At high temperatures, there are still unanswered problems about creep and creep fatigue crack formation for which data is desperately required, particularly for irradiated metals that have elevated Helium concentrations.

NFAs' inclination for micro cracks and lamination results from the formation of the robust  $\{100\}\langle 011\rangle$ -cleavage-system appearance, which was previously seen in Fig. 1a. In certain circumstances, such patterning makes NFA displacement detection quite challenging. Based on the observed elastic fracture pressures under tensile loading corresponding to the (100) planes and presuming a limits penny-shaped microcrack with a radius of  $60\text{ }\mu\text{m}$ , the



estimated  $\{100\}\langle 011 \rangle$ -splitting KIC is under ten MPa $\sqrt{\text{m}}$  at the average temperature. As shown by an approach to theoretical strength as well as tensile characteristics, the  $\{100\}\langle 011 \rangle$ -splitting KIC rises quickly beyond ambient temperatures in accordance with the master curve, and the appropriate BDTT is calculated to be  $\approx 100^\circ\text{C}$ . The NFA-1 plate's pre-existing microcracks in other words, do not easily spread to result in lamination and significant ductility loss above this BDTT. This is important since it indicates that treating deformation at temperatures higher than those is preferred. Interpreting the mathematics of the master curve, especially variations brought on by radiation, is significantly impacted by these findings on basic cleavage fracture in a high toughness alloy. Furthermore, at the dislocation level, the fundamental processes behind the texturing and tiny cracks of the  $(100)\langle 011 \rangle$  cleavage system have become well characterized. Nevertheless, further in-depth examination of these fascinating subjects is beyond the purview of this essay.

#### **E. Tolerance for Radiation**

The following are the primary causes of NFAs, which' distinct irradiation tolerance in comparison to 9Cr tempered martensitic steels (TMS) : NFAs should have smaller BDTT shifts because they harden less than regular TMS at irradiation temperatures below around  $400^\circ\text{C}$ . NFAs maintain a sizable homogenous stress and cracking capacity in comparison with TMS. The linked causes are thought to be: a) enormous mathematically necessary dislocating density stages, ranging mainly linked to smaller NFA grain sizes, which increase strengthening rates while lowering flow localisation; and b) mixture impacts of the NOs' noteworthy impact on unirradiated highlights on yield, which reduce the net hold define rectangular funding from irradiation-induced barriers. Although the exact process is unknown, enhanced combination by NO defect trapping could additionally decrease ray hardening via dislocation loops and precipitation. In contrast to when they are linked to NOs in NFAs, hydrogen particles, which increased the dpa and temperatures of hardness in traditional TMS, had a smaller hardening contribution. These processes more than compensate for the hardening effects of the radiation-enhanced diffusion-accelerated  $\alpha'$  condensation that takes place in NFAs.

NFAs have a good resistance to void enlargement at lower temperatures. NFA swelling obstruction, in contrast to TMS, endures despite the elevated He levels seen in fusion settings. Once again, the cause is because

he is imprisoned at NO borders in microscopic bubbles. The tiny bubbles are far smaller than what is required for them to transform into voids that expand unsteadily. Furthermore, because of the tiny grain sizes, the He that crosses particle borders is less condensed.

In NFAs, he control is crucial because it avoids embrittlement linked to large, rapid fracture BDTT changes that happen in traditional TMS at low to the middle irradiation degrees. At elevated He levels, these BDTT changes may escalate to hundreds of degrees Celsius. These significant changes result from the combined impact of He-weakened boundaries of grains and irradiation hardness. The possibility of more severe cracking, which might be reflected in decreased creep rupture durations and stresses linked to stress-driven formation of grain boundary cavities that nucleation on critically large He a bubble is also reduced by trapping He at NOs. One unresolved problem is how He affects creep and creep-fatigue crack development. Treatment creep rates in NFAs are often only somewhat less than those in traditional 9Cr TMS. On the other hand, a large concentration of He-bubble sinks is predicted to reduce irradiation creep.

#### **F. Synopsis of the Research**

Over the preceding decade, NFA the physical, mechanical, and photonic research into materials has advanced dramatically. Maintaining NFA micro-nanostructures and maintaining their outstanding properties are well known till compaction. So, we know how NFAs operate. Regretfully, while we are capable of creating excellent NFAs, we are still learning how to fully use them for engineering purposes.

#### **3. NFA Component Fabrication and Joining**

Isostatic hot pressing (HIP) or spark plasma annealing may consolidate powder-processed NFA parts towards net form. NFA programs, typically comprise thin plates and laminating tubing with significant in-plane characteristics, may need deformation modifications. The high endurance, anisotropy the microscope, and potent crystalline structuring of macro-defect-free NFAs make device shaping difficult. Although micro-nanostructures have excellent NFA efficiency, bent treatments must limit their very asymmetrical creep and fracturing. A) developing thin-walled tubing involves cold building, intermediate heating decreasing, and high temperatures recovery-recrystallization; and b) cross-rolling as-extruded bills to create plates. It is impossible for this brief study to adequately address the core

fundamental mathematics and highly technical issues that deformation processing faces. There are outstanding evaluations of this subject in and for a cross-rolled plate. As previously mentioned, one of the main concerns when manufacturing components free of defects is the fact that certain deformation production pathways result in the production of unstable cleavage fracture systems.

Though scientific understanding has begun to appear in very impressive ways, the thermomechanical manufacturing of certain crucial NFA types remains a mostly unresolved difficulty. This is the most significant takeaway that can be drawn from the writer's own experiences and a review of the scientific literature. Reduced Cr, C-bearing convertible metals are more fabricable than the NFAs, which may partially make up for their somewhat lower hardness as well as efficiency capability. There is evidence that hot hydraulic extrusion thin-walled NFA cylinders may be without any flaws and that particular blasting heating processes can reduce cross-rolled plate fracture minuscule splitting. Therefore, it is advised to "stay tuned" while discussing distortion processing NFAs. Although there isn't enough room to talk about it either, strong connecting of NFA parts is a realistic and doable objective. Solid-state joining methods, including as dispersion connecting, pressure resisting upset welding because and friction stir welding (FSW), are required. Maintaining the NOs in an area of significant plastic deformation is a key concern in the FSW situation.

However, recent attempts to solve FSW methods and variables such as tool rotational velocity, should handle several complicated issues. Furthermore, this field has interesting publications. Certain applications, such as joining NFAs and TMS, will call for dissimilar metal junctions. Although diffuse bonding would appear to be the most appealing option for this kind of application, there may be serious problems with C transfer, and in some situations, multilayer obstacles may be necessary for the steel-to-steel connections. In some situations, brazing may also be used to join. Bonded NFAs to W for fusion reactors divertor usage is a more difficult problem because of the wide temperature swings and differences in their coefficients of expansion due to heat.

#### **4. NFA industrial scaling, cost, economic supplies capability, and applications**

One of the several studies mentioned suggests that the best NFA would require powder synthesis by metallic alloying and hot aggregating process. With prealloyed powders, which phase split when melted and re-

solidified, this requirement may rule out otherwise alluring technological additive solutions. Due to their extreme hardness, milling powders are challenging to cold spray. On the other hand, ODS alloys with larger oxides, reduced strength, and ultraviolet tolerance could be suitable for the procedures. Deforming NFAs into delicate, flawless geometries like thin-walled tubes while keeping or improving their structural and operation properties may be possible with future fundamental and application study.

However, raw material NFAs and Organic pollutants iron production will be costly. Expenses constantly raise the question of who will make NFAs and ODS materials and why. No matter how severe the need, applications are not limited to nuclear energy and fission. Granular metallurgy-based nano-dispersion hardened materials are used in chemicals, electricity, transportation, and aviation. However, developing use requires a supplier, and suppliers require an outlet for apps.

The creator of this Opinion article is hopeful that a supplier of NFA/ODS metal will emerge and that a market for a wider range of nanooxide dispersal strengthening alloys, such as those composed of Ti, Ni, Al, Mg, and refractory metals like W, will grow in tandem. These need to feature unique specialised uses for everyday goods. Therefore, costly, high-strength NFAs won't be used for heavy section constructions or various applications needing a lot of material. Instead, they would be employed as very challenging, small-volume parts of intricate multimaterial system designs.

According to a major industrial provider of ball-milled powders and attritor mills, it would be feasible to increase NFA output to 1000 metric tonnes annually, which would enable it to reach the \$50/kg goal price for combined billets required for many different use. The use of NFAs as a 5 mm thick layer in a fusion reactor first wall and divertor hybrid construction architecture may provide insight into expenses since it is strong, wear resistant, and radiation tolerant. For a big demonstration fusion reactor, which would cost around 50 million dollars at the billet price mentioned above, this would need roughly 104 kg of NFA. Naturally, this excludes the fabrication costs of an NFA structure, which are likely to be more than those of a TMS-based system with inferior performance, even though the latter would most likely need a post-weld heat treatment. However, it is anticipated that the additional expense of a performance-enabling NFA hybrid superstructure will only make up a minor portion of the roughly \$10 billion cost of a fusion power reactor. For instance, a first wall fusion structure



costs less than 180 million dollars, compared to pressurised water-cooled nuclear reactor steam engines, which are just a small part of a nuclear plant's pressure boundary. Naturally, the cost of installation does not account for the many other aspects of electric power economics, such as waste management, environmental effect, element lifespan, efficiency, and safety.

## 5. Conclusions

This paper highlights a major achievement in the field of materials science, the rapid progress made in the scientific foundation for developing nanostructured alloys. These alloys show excellent mechanical properties, high-temperature stability, and outstanding resistance to radiation, making them ideal for demanding environments such as advanced energy systems like fusion and fission reactors. Despite all these developments, the industrial process for defect-free nanostructured alloy components is still under development, requiring further refinements in material design and fabrication techniques to achieve their optimal performance and longevity.

Oxide dispersion-strengthened (ODS) variations of 9Cr tempered martensitic steels (TMS) represent a promising alternative, which can overcome many of the challenges related to nanostructured alloys. The materials show better manufacturability and reliability with a modest performance compromise. They can withstand extreme conditions and remain structurally sound, making them a practical candidate for high-temperature applications. Still, the scalability and cost-effectiveness of nanostructured alloys and ODS TMS for large-scale deployment are uncertainties. These issues remain critical barriers to their adoption in advanced engineering systems. The present study does not solve all these challenges, but it is able to provide an in-depth performance and longevity analysis of nanostructured alloys with potential pathways to industrial application. With the progressive development of material science and manufacturing technology, the hope is to overcome these challenges in order to take nanostructured alloys to a leading role in the high-temperature, next-generation energy systems.

## References

- [1] S.J. Zinkle, G.S. Was, *Acta Mater.* 61 (2013) 735-758.
- [2] G.R. Odette, M.J. Alinger, B.D. Wirth, *Ann. Rev. Mater. Res.* 38 (2008) 471-503.
- [3] G.R. Odette D.T. Hoelzer, *JOM* 62 9 (2010) 84-92.
- [4] Avacharmal, R., Pamulaparthivenkata, S., Ranjan, P., Mulukuntla, S., Balakrishnan, A., Preethi, P., & Gomathi, R. D. (2024, June). Mitigating Annotation Burden in Active Learning with Transfer Learning and Iterative Acquisition Functions. In 2024 15th International Conference on Computing Communication and Networking Technologies (ICCCNT) (pp. 1-7). IEEE.
- [5] Suresh, K., Reddy, P. P., & Preethi, P. (2019). A novel key exchange algorithm for security in internet of things. *Indones. J. Electr. Eng. Comput. Sci.* 16(3), 1515-1520.
- [6] S.J. Zinkle, J-L Boutard, D.T. Hoelzer, A. Kimura, R. Lindau, G.R. Odette, M. Rieth, L. Tan, H. Tanigawa, *Nuclear Fusion* (2017).
- [7] T.K. Kim, S. Noh, S.H. Kang, J.J. Park, H.J. Jin, M.K. Lee, J. Jang, C.K. Rhee, *Nuc. Eng. and Tech.* 48 2 (2016) 572-594.
- [8] S. Ukai, *Comprehensive Nuclear Mater.* Elsevier (2012) 241-271.
- [9] S. Ukai, S. Ohtsuka, T. Kaito, Y. de Carlan, J. Ribis and J. Malaplate, *Structural Materials for Generation IV Nuclear Reactors*, Ch. 10 Elsevier (2017).
- [10] M.J. Alinger, G.R. Odette, D.T. Hoelzer, *Acta Mater.* 57 (2009) 392-406.
- [11] Ansari, S. A., & Zafar, A. (2023, March). A Comprehensive Study on Video Captioning Techniques, Benchmark Datasets and QoS Metrics. In 2023 10th International Conference on Computing for Sustainable Global Development (INDIACom) (pp. 1598-1603). IEEE.
- [12] M.J. Alinger, G.R. Odette, D.T. Hoelzer, *J. Nuc. Mater.* 329-333 (2004) 382-386.
- [13] N.J. Cunningham, Ph.D. Dissertation, University of California Santa Barbara (2012).
- [14] N.J. Cunningham, Y. Wu, D. Klingensmith, G.R. Odette, *Mat. Sci. Eng. A* 613 (2014) 296-305.
- [15] Preethi, P., & Asokan, R. (2019). A high secure medical image storing and sharing in cloud environment using hex code cryptography method—secure genius. *Journal of Medical Imaging and Health Informatics*, 9(7), 1337-1345.
- [16] P. Dou, A. Kimura, R. Kasada, T. Okuda, M. Inoue, S. Ukai, S. Ohnuki, T. Fujisawa and F. Abe, *J. Nuc. Mater.* 444 1-3 (2014) 441-453.

- [17] J.R. Rieken, I.E. Anderson, M.J. Kramer, G.R. Odette, E. Stergar, E. Haney, J. Nuc. Mater. 428 1-3 (2012) 65-75.
- [18] N.J. Cunningham, Y. Wu, A. Etienne, E.M. Haney, G.R. Odette, E. Stergar, D.T. Hoelzer, Y.D. Kim, B.D. Wirth, S.A. Maloy, J. Nuc. Mater. 444 1-3 (2014) 35-38.
- [19] L. Barnard, N.J. Cunningham, G.R. Odette, I. Szlufarska, D. Morgan, Acta Mater. 60 3 (2012) 935-947.
- [20] L. Yang, Y. Jiang, Y. Wu, G.R. Odette, Z. Zhou, Z. Lu, Acta Mater. 103 (2016) 474-482.

